Journal of Colloid and Interface Science 363 (2011) 595–600

Contents lists available at SciVerse ScienceDirect

Journal of Colloid and Interface Science

www.elsevier.com/locate/jcis

Effects of electrolyte concentration and counterion valence on the microstructural flow regimes in dilute cetyltrimethylammonium tosylate micellar solutions

N. Tepale [a], E.R. Macías [b], F. Bautista [b], J.E. Puig [b], O. Manero [c], M. Gradzielski [d], J.I. Escalante [e,*]

[a] Chemical Engineering Department, Benemérita Universidad Autónoma de Puebla, Puebla 72520, Mexico
[b] Chemical Engineering Department, Universidad de Guadalajara, Boul. M. García Barragán # 1451, Guadalajara, Jalisco 44430, Mexico
[c] Materials Research Institute, Universidad Nacional Autónoma de México (UNAM), Apdo. Postal 70-360, México City, DF 04510, Mexico
[d] Stranski-Laboratorium für Physikalische und Theoretische Chemie, Institut für Chemie, Technische Universität Berlin, Straße des 17. Juni 124, Sekr. TC7, D-10623 Berlin, Germany
[e] Chemistry Department, Universidad de Guadalajara, Boul. M. García Barragán # 1451, Guadalajara, Jalisco 44430, Mexico

ARTICLE INFO

Article history:
Received 10 May 2011
Accepted 18 July 2011
Available online 5 August 2011

Keywords:
Generalized dynamic diagram
Ionic strength
Micellar solutions
Shear-induced structures
Shear thickening

ABSTRACT

The shear thickening behavior and the transition to shear thinning are examined in dilute cetyltrimethylammonium tosylate (CTAT) micellar solutions as a function of surfactant concentration and ionic strength using electrolytes with different counterion valence. Newtonian behavior at low shear rates, followed by shear thickening and shear thinning at higher shear rates, are observed at low and intermediate surfactant and electrolyte concentrations. Shear thickening diminishes with increasing surfactant concentration and ionic strength. At higher surfactant or electrolyte concentration, only a Newtonian region followed by shear thinning is detected. A generalized flow diagram indicates two controlling regimes: one in which electrostatic screening dominates and induces micellar growth, and another, at higher electrolyte and surfactant concentrations, where chemical equilibrium among electrolyte and surfactant counterions controls the rheological behavior by modifying micellar breaking and reforming. Analysis of the shear thickening behavior reveals that not only a critical shear rate is required for shear thickening, but also a critical deformation, which appears to be unique for all systems examined, within experimental error. Moreover, a superposition of the critical shear rate for shear thickening with surfactant and electrolyte concentration is reported.

1. Introduction

Dilute micellar solutions exhibit shear thickening behavior at concentrations around the sphere-to-rod micellar transition (cmc_2) due to the formation of shear-induced structures (*SIS*) [1,2]. This flow phenomenon is characterized by a Newtonian regime at low shear rates (or stresses), followed by a drastic viscosity increase at shear rates (or stresses) equal or larger than a critical value $\dot{\gamma}_c$ (or σ_c), while at even larger shear rates (or stresses), shear thinning arises [3]. This flow phenomenon is not exclusive of dilute micellar solutions, since it has been reported for a variety of systems, such as colloidal dispersions [4], microemulsions [5], concentrated suspensions [6] and associative polymer solutions [7].

In the shear thickening regime, two characteristic times are observed: an induction time (t_{ind}) required to produce the formation of *SIS*, which may range from seconds to minutes, depending on how much larger is the applied shear rate (or stress) compared to $\dot{\gamma}_c$ (or σ_c), and a saturation time (t_{sat}), required for the *SIS* development and the attainment of the steady state viscosity [8–10]. Both the induction and saturation times detected by rheometry coincide with those observed by flow birefringence [9] and small-angle light scattering under flow [11]. Both times become shorter as the applied shear-rate departs from $\dot{\gamma}_c$ and they depend on temperature, surfactant concentration and on the thermal and shear histories of the sample [12,13].

Hu et al. [8] reported that in the shear thickening regime for dilute surfactant solutions subjected to different shear stress at steady state conditions, there are four different types of behavior. At low shear stresses (smaller than σ_c) or shear rates (smaller than $\dot{\gamma}_c$), the solution is Newtonian with a viscosity equal or slightly larger than that of the solvent (Region I), although shear thinning has also been observed in some systems [14–17]. Region II occurs for intermediate shear stresses, where a re-entrant region is detected at intermediate values ($\sigma_c < \sigma < \sigma_s$) only under stress-controlled conditions and shear thickening develops [8,18–21]. In Region III, for $\sigma_s < \sigma < \sigma_f$ (see Fig. 2 for more details), the apparent viscosity keeps increasing but the $\sigma - \dot{\gamma}$ flow curve increases now monotonically, and the *SIS* are produced by homogeneous nucleation; in these regions, coexistence of a shear-induced gel-like oriented phase and a homogeneous fluid phase containing the original rod-like micelles has been proposed, as suggested by light

* Corresponding author. Fax: +52 33 13785900 27534.
E-mail address: escalant@hotmail.com (J.I. Escalante).

0021-9797/$ - see front matter © 2011 Elsevier Inc. All rights reserved.
doi:10.1016/j.jcis.2011.07.051

scattering [8,22]. For $\sigma > \sigma_f$, the *SIS* break down mechanically [22] or the wormlike micelles align with the direction of the flow [23] and shear thinning occurs (Region IV). Macías et al. [10] also identified these four flow regions with a stress-controlled rheometer and flow visualization by particle image velocimetry (PIV) in dilute CTAT aqueous solutions; here shear thickening occurred without a re-entrant region.

The addition of electrolytes to micellar solutions of ionic surfactants can induce micellar growth as a consequence of electrostatic screening [24–29], thereby increasing substantially the viscosity. When organic salts with strongly binding counterions such as sodium tosylate or salicylate, are added to ionic solutions of cationic surfactants such as cetyltrimethylammonium bromide (CTAB), the concentration regime at which elongated micelles form, shifts to even lower surfactant concentrations [2,22,30]. Accordingly, surfactants with strongly binding counterions, such as CTAT, can form elongated cylindrical micelles at concentrations much lower than common surfactants, such as CTAB, without the addition of electrolytes [31,32], and so, shear thickening behavior arises at these low concentrations [10,23].

Even though there are several reports on shear thickening in ionic surfactant micellar systems upon addition of electrolytes [3,15,33–37], there is no systematic examination of the electrostatic screening and the chemical equilibrium interactions between the surfactant and the electrolyte counterions, particularly with surfactants containing strongly binding counterions such as CTAT. However, this is a central aspect for the control of the flow behavior in surfactant systems as it is often important in practical applications.

In this work, the effects of adding electrolytes with different counterion valence on the shear thickening behavior and the transition to shear thinning in dilute CTAT solutions are investigated. Here it is shown that all the effects of electrolytes on dilute micellar solutions of surfactants with strongly binding counterions can be cast into a generalized flow diagram, where the rheological behaviors and the mechanisms involved are indicated. Further analysis of shear thickening indicates that not only a critical shear rate with a concomitant induction time are required for shear thickening, but also a critical deformation, which is the same for all systems examined. These issues may be crucial for many applications and formulation processes because salts are naturally present, and because the potential of controlling the rheological behavior of surfactant solutions by the proper choice of added salts. In particular, in many formulation processes high shear is applied to surfactant systems for certain periods of time for homogenization or processing and accordingly, the response of surfactants system to such external impacts is of high importance.

2. Experimental section

CTAT, 99% pure from Sigma, was re-crystallized from a chloroform (Aldrich) solution before using it. KBr, $Na_2(COO)_2$ and K_3PO_4, with a purity of 99% from Fermont, were used as received. HPLC-grade water was employed.

For CTAT/salt/water solutions, two schemes of rheological measurements were performed: in the first one, the electrolyte concentration was fixed at 10^{-4}, 10^{-3}, 10^{-2} or 10^{-1} mol/L and the surfactant concentration was varied; in the second one, the surfactant concentration was fixed (11 mmol/L) and the electrolyte concentration was varied. Salt solutions were made by diluting 0.1 mol/L stock solutions of the respective electrolyte. Samples were prepared by weighing the appropriate amounts of surfactant and water or electrolyte solution in 20-mL glass vials, homogenized and placed in a temperature-controlled chamber at 30 °C for a week before performing the rheological tests.

Steady and transient shear rate measurements were performed at 30 ± 0.1 °C using two instruments: an ARES strain-controlled rheometer equipped with a double-wall Couette geometry with bob inner and outer diameters of 29.5 mm and 32 mm, respectively, and cup with D_i = 27.94 cm and D_o = 34 cm; and a Rheometrics SR5 strain-controlled rheometer equipped with a cone-and-plate geometry (0.0384°-angle and 4 cm-diameter). To minimize water evaporation, a homemade humidification chamber was set around the cone-and-plate device. Measurements for all samples were performed as follows: first the sample was placed in the shear cell where it was allowed to stand still for about 5 min, before starting the experiment to eliminate any shear history. Moreover, since the micellar solutions prepared with the different salts had a pH-dependence due to the dissociation kinetics of the electrolytes, the measurements were performed until the samples reached equilibrium (for example, K_3PO_4 solutions mainly contain HPO_4^{2-} counterions at a pH of 8 due to the pK_a's of this salt, whereas $Na_2(COO)_2$ and KBr solutions at a pH of 6.5 contain $(COO)_2^{2-}$, and Br^- counterions).

3. Results and discussion

Fig. 1 depicts steady shear flow curves of dilute CTAT micellar solutions as a function of surfactant concentration at a fixed electrolyte concentration (10 mmol/L) measured in the SR-5 strain-controlled rheometer at 30 °C. This figure indicates that two distinct flow regimes develop as the surfactant concentration is increased above the cmc_2, which is ca. 1 mmol/L CTAT in water (0.045 wt.%) at 30 °C [31]. Unfortunately, no data about the cmc_2 are available in the literature for CTAT in the presence of electrolytes, however, the cmc_2 should diminishes with increasing electrolyte concentration, as expected for another anionic surfactants. For CTAT concentrations lower than ca. 17.6 mmol/L, Newtonian behavior at low shear rates followed by shear thickening at intermediate shear rates, and by incipient shear thinning at higher shear rates, were detected, within the shear rate range

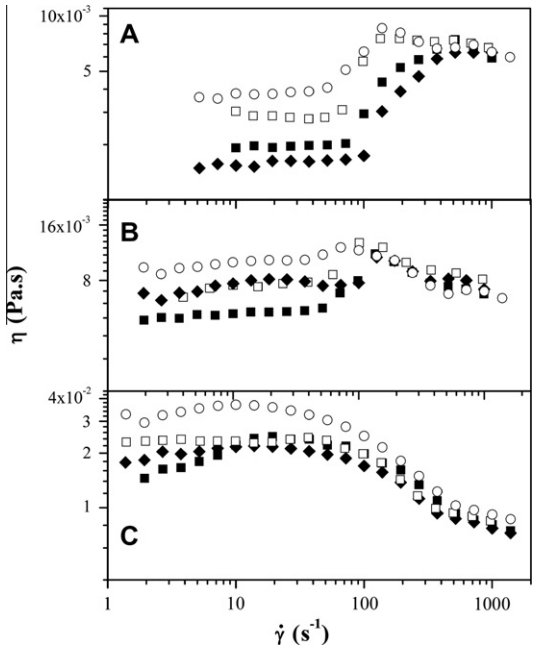

Fig. 1. Apparent viscosity as function of shear rate for micellar solutions containing salt (■) KBr, (♦) K_3PO_4, (○) $Na_2(COO)_2$ and no salt (□). The electrolyte concentration in all these solutions was 0.1 mmol/L, and the CTAT concentration was varied: (A) 11 mmol/L, (B) 17.6 mmol/L, and (C) 22 mmol/L.

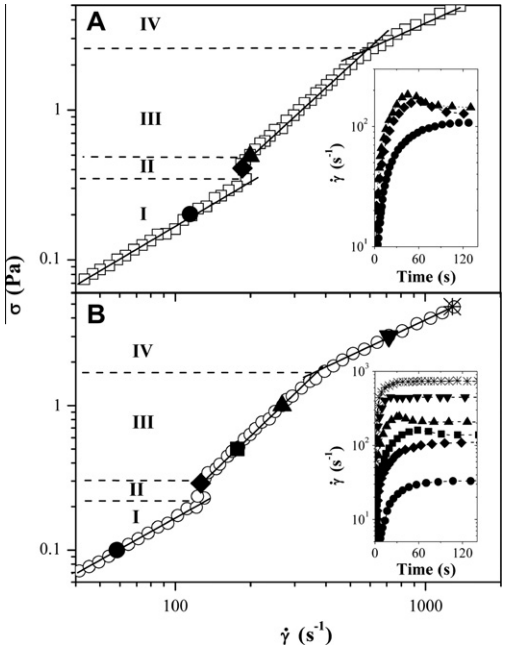

Fig. 2. Shear stress versus shear rate for micellar solutions containing 8.8 mmol/L CTAT and 0.1 mmol/L electrolyte: (A) CTAT/KBr, (B) CTAT/$Na_2(COO)_2$. Inset: Shear rate growth at constant shear stress, where the corresponding symbols are indicated in the shear flow curve.

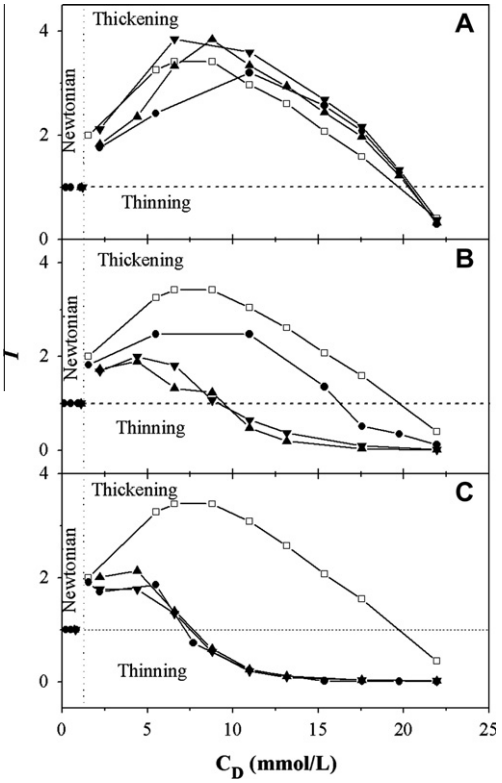

Fig. 3. Shear thickening intensity, *I*, as function of CTAT concentration for various electrolyte concentrations and type: (A) 0.1 mmol/L, (B) 1 mmol/L and (C) 10 mmol/L: (□) without salt, (●) KBr, (▲) $Na_2(COO)_2$ and (▼) K_3PO_4.

examined (Fig. 1A); at slightly higher CTAT concentrations, similar behavior than that reported in Fig. 1A was observed, but with more pronounced shear thinning at higher shear rates, regardless of the electrolyte type (Fig. 1B). Notice that as surfactant concentration is increased, shear thickening diminishes (Fig. 1B), and at higher electrolyte concentrations, only a Newtonian regime followed by shear thinning is observed (Fig. 1C). Clearly, the transition between shear thickening and shear thinning regimes is not abrupt. In fact, the shear thickening intensity ($I = \eta_{MAX}/\eta_0$) diminishes steadily as the surfactant concentration is increased, until it becomes one, indicating that shear thickening has disappeared at surfactant concentrations around 19 mmol/L (ca. 0.85 wt.%) in the absence of electrolyte; here η_{MAX} and η_0 are the maximum viscosity achieved during shear thickening and the zero-shear rate viscosity, respectively, at each CTAT concentration.

Fig. 2 displays the steady-state shear stress versus shear rate curves for micellar solutions containing 8.8 mmol/L (0.4 wt.%) CTAT and 0.1 mmol/L electrolyte: CTAT/KBr (Fig. 2A), and CTAT/$Na_2(COO)_2$ (Fig. 2B). Both curves are alike, in which four regions similar to those reported elsewhere [18,22], are clearly distinguishable (indicated in Fig. 2A and B). It is important to notice that the flow curves shift to lower shear rates with increasing electrolyte counterion valence (cf. Fig. 2A and B). In fact, with K_3PO_4, the shift is even more pronounced (not shown), which is not surprising inasmuch as electrostatic screening should increase with increasing counterion valence yielding shear thickening at lower shear rates, since SIS can be induced more easily due to reduced electrostatic repulsion. The inset in Fig. 2 represents the shear rate growth experiments made at constant shear stress where the corresponding symbols are plotted in the shear flow curve, and which show that a steady-state is typically attained after about 20–100 s. Notice that for shear rates smaller than $\dot{\gamma}_c$ or high shear rates (Region IV), all solutions behave like Maxwell fluids with a single relaxation time. However, for shear rates in Regions II and III, overshoots and oscillations develop, which indicates that the micellar solutions have several relaxation times [38].

Fig. 3 shows plots of *I* versus surfactant concentration (C_D) for the electrolytes used at several concentrations; for comparison purposes, rheological data in the absence of electrolyte are included. A common feature of the plots, not shown in Fig. 3, is that at surfactant concentrations smaller than ca. the cmc_2 (1 mmol/L), Newtonian behavior is observed regardless of electrolyte type and concentration. For concentrations larger than the cmc_2, electrolyte concentration and counterion valence influence the rheological behavior. At low electrolyte concentrations (Fig. 3A), all samples exhibit similar shear thickening behavior along the entire surfactant concentration range: *I* increases with surfactant concentration up to ca. 7 mmol/L, where a maximum is detected and then it diminishes below one at $C_D \approx 20$ mmol/L, indicating that only shear thinning is occurring. The C_D at which the transition from shear thickening to shear thinning occurs ($I = 1$) is referred therein as the critical surfactant concentration.

Examination of Fig. 3A–C suggests a general ordering of the electrostatic screening effect of the electrolyte counterions on the shear thickening as $PO_4^{3-} > (COO)_2^{2-} > Br^-$. Notice, however, that at low electrolyte concentration (Fig. 3A), a definitive effect of the electrolyte type on the shear thickening intensity is not apparent. However, for electrolyte concentrations higher than 0.1 mmol/L, larger electrostatic interactions between micelles and the electrolyte counterions develop, which strongly depend on the counterion valence (Fig. 3B). Apparently the valency of the counterion has a significant effect on the micellar structures formed under shear and thereby on their flow behavior. Samples without electrolyte and with KBr have a shear thickening behavior similar to that described in Fig. 3A, although the presence of KBr diminishes *I* compared to that in absence of electrolyte, whereas samples with $Na_2(COO)_2$ and K_3PO_4 exhibit much smaller *I*-values and the critical surfactant concentration shifts to lower values. At even higher electrolyte concentrations (Fig. 3C), the shear thickening region has

almost disappeared for all salts, and the critical surfactant concentration shifts to even lower values. Incidentally, for electrolyte concentrations larger than ca. 100 mmol/L, no shear thickening behavior was detected in the whole surfactant concentration range, only a Newtonian behavior at low surfactant concentrations followed by shear thinning was detected (not shown). Apparently at such high ionic strength, no further shear-induced growth of wormlike micelles can take place.

Data shown in Fig. 3 for the different electrolyte concentrations employed can be set in a generalized diagram by plotting the normalized shear intensity, $(I-1)/(I_{max}-1)$, (being I_{max} the maximum shear thickening intensity at a given electrolyte concentration) versus the normalized surfactant concentration, C_D/C_{Dmax}, where C_{Dmax} is the surfactant concentration at which I_{max} occurs. The plot was built in this way because it allows defining the mechanism that controls the shear thickening transition, i.e., micellar growth by electrostatic screening or micellar scission or branching and/or scission-reformation due to chemical equilibrium among surfactant molecules and added electrolyte, and the transition from shear thickening to pure shear thinning behavior ($(I-1)/(I_{max}-1)=0$ in Fig. 4). Within experimental error, all data collapse in the shear thickening region, exhibiting a quadratic master curve that limits the four regimes observed in the transition from shear thickening to the shear thinning regime. At very low surfactant concentrations ($C_D/C_{Dmax}\to 0$), a Newtonian regime is detected at the left side of the diagram, whereas the shear thickening region is found next, and at higher C_D/C_{Dmax} (>2.2), the shear thinning region appears. At very high C_D/C_{Dmax}, another Newtonian region is detected.

The interpretation of this diagram is that at low surfactant concentrations upon increasing electrolyte concentration, micelles grow due to electrostatic screening and the shear thickening flow regime develops. However, once micelles have grown to wormlike micelles, shear thinning occurs. In this regime, electrolytes diminish shear thinning by modifying the kinetics of scission or by allowing branching due to chemical equilibrium among the surfactant counterions and the electrolyte counterions. It can be speculated that the presence of the electrolyte stabilizes intermediate structures during the scission process, thereby facilitating this process. Notice that this diagram allows defining the boundary between the pure shear thickening, the shear thickening-to-shear thinning transition, and the pure shear thinning regions. Incidentally, to demonstrate that these rheological behaviors may be general, rheological data of surfactants with strongly binding counterions in the presence of electrolytes, taken from the literature [3,33,36,37], are also included in this figure and fall onto the same master curve.

Takeda et al. [39] also reported a flow behavior diagram in the CTAB/sodium p-toluene sulfonate (NapTS) system as a function of the ratio of C_D and of C_{Salt}/C_D in which five regions were detected by Rheo-SANS, mainly purely Newtonian where spherical micelles are present, Newtonian followed by shear thickening due to formation of short rod-like micelles, shear thinning followed by shear thickening where rod-like and wormlike micelles coexist, shear thinning due to alignment of wormlike micelles, and precipitation regions. Moreover, their interpretation of such flow diagram is quite similar to the one presented here, except that no precipitation region was observed by us.

Fig. 5 depicts the dependence of the critical shear rate $\dot{\gamma}_c$ on surfactant concentration in the presence of 0.1 mmol/L KBr, $Na_2(COO)_2$ or K_3PO_4. Even though the data are scattered, a power law dependence of $\dot{\gamma}_c$ with C_D ($\dot{\gamma}_c \propto C_D^{\alpha}$) is apparent. The straight line in this plot is the best power-law fit to the data with $\alpha = -0.87 \pm 0.2$. In general, the critical shear rate for shear thickening depends weakly on surfactant concentration [10,32,40,41]. For instance, values of $\alpha = -0.55 \pm 0.05$ have been reported for CTAT in D_2O [36], $\alpha \approx 0$ for CTAT in H_2O [10,42] and CTAVB in H_2O [32]. In dilute micellar solutions of a 12-2-12 gemini cationic surfactant [37], $\dot{\gamma}_c$ also shifts to lower values upon increasing surfactant concentration but no value of the exponent α was reported. An explanation for the larger exponent α of CTAT micellar solutions in the presence of electrolytes could be the pronounced growth of the micellar length with increasing concentration. It is noteworthy that the data presented here suggest again that electrostatic screening is less important when the micelles are composed of surfactants with strongly-binding counterions, such as tosylate; hence, no strong effect of the electrolyte counterion valence is noticed. It is also interesting that both $\dot{\gamma}_c$ and I decrease as C_D increases (Figs. 3–5).

It is well known that in dilute surfactant solutions, the shear thickening transition (*STT*) occurs at concentrations where cylindrical micelles locally exist, as deduced by SANS experiments of quiescent solutions [40], i.e., from the cmc_2 up to the neighborhood of the overlap concentration c^*. The latter concentration marks the sharp increase of the zero-shear rate viscosity due to the incipient entanglement formation among wormlike micelles. Hence, it is likely that the intensity of the shear field required to induce

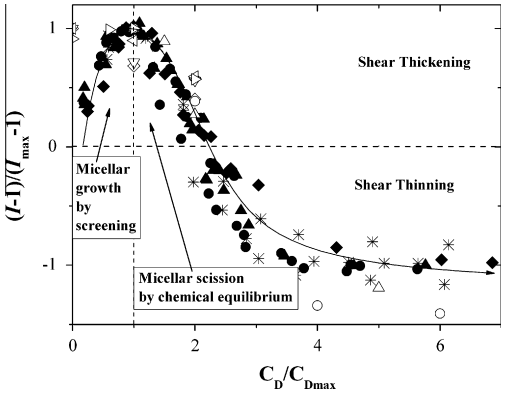

Fig. 4. Generalized diagram of normalized shear thickening intensity as function of normalized surfactant concentration for various electrolyte concentrations and type: (✳) without salt, (♦) KBr, (▲) $Na_2(COO)_2$ and (●) K_3PO_4. Rheological data from strongly binding counterions from literature: (△) CTAT/D_2O/NaCl [36], (○) CTAB/NaSal/NaCl [3], (◇) CTAB/NaSal/$NaNO_3$ [3], (▽) CTAB/NaSal/NaF [3], (◁) Gemini surfactant [37] and (▷) CTAT/H_2O/NaCl [33]. The solid lines are only guides to the eye.

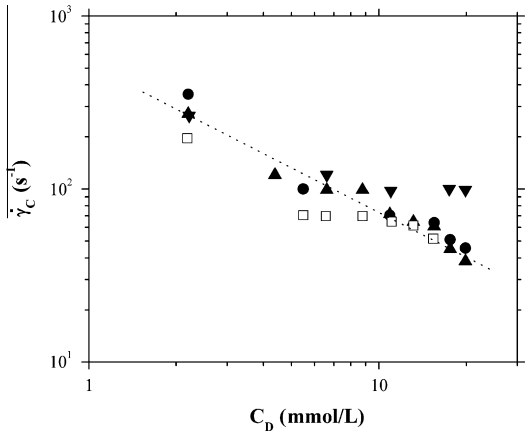

Fig. 5. Critical shear rate for shear thickening as function of surfactant concentration for micellar solutions containing (□) CTAT, (●) CTAT + KBr, (▲) CTAT + $Na_2(COO)_2$ and (▼) CTAT + K_3PO_4. The electrolyte concentration in all these solutions is 0.1 mmol/L.

structure formation needs to be larger at low surfactant concentrations, where mostly rodlike micelles exists, than at larger concentrations, where rodlike and wormlike micelles coexist. This should explain why the critical shear rate for *STT* diminishes with increasing surfactant concentration. However, at low electrolyte concentrations, the electrostatic screening, regardless of the counterion valence, is not that important for surfactants such as CTAT due to the strong binding of the organic counterions to the micelle surface. In fact, Truong and Walker [41] demonstrated by a combination of static light scattering, small-angle neutron scattering and rheological measurements, that the shear-induced structural transition in dilute CTAT micellar solutions disappears with increasing NaCl concentration once the intermicellar electrostatic interactions are adequately screened; however, they had to add relatively large amounts of NaCl to produce this effect, in agreement with the results reported here (see Fig. 4).

As expected from the data in the literature [8–10], the induction time of the CTAT micellar solutions, defined here as the time at which the viscosity begins to increase at a given shear rate, follows a power law relationship of the form, $t_{ind} \propto \dot{\gamma}^m$, with the various electrolytes added; in particular, for a 11 mmol/L CTAT solution, the exponent m is equal to -2.3 ± 0.30, -2.6 ± 0.01, -2.1 ± 0.30 and -3.2 ± 0.20, for no electrolyte, KBr, $Na_2(COO)_2$ and K_3PO_4, respectively (see Table 1). Similar power laws have been reported for other surfactant systems with exponents ranging from -1 to ca. -3 [8–10]. Moreover, the value of m depends on the geometry employed as pointed out before [10]. In our case no systematic dependence of m on the counterion valency is observed and this applies similarly for the induction time t_{ind}, which is a bit surprising as one might expect the onset of micellar growth to depend on the extent of electrostatic screening (while in our case this time is even longest for the K_3PO_4).

Since the induction time decreases with increasing shear rate when $\dot{\gamma} > \dot{\gamma}_c$, it is interesting to explore whether a unique shear strain is required for the formation of *SIS* that produce shear thickening. Table 1 discloses that as $\dot{\gamma}_c$ increases, the induction time becomes shorter, which suggests that a unique deformation is required to produce shear thickening. Defining the critical shear strain as γ_c $(= \dot{\gamma}_c t_{ind,c})$, reveals that a unique deformation, within experimental error, is required for the development of SIS for all the systems studied here, which leads to viscosity increase with time (Table 1). This is the first time that a unique shear strain has been reported for dilute micellar solution. A similar finding was previously reported by Escalante et al. for the rheological behavior of pristine lamellar phases that undergo a transition to vesicles under shear for a series of alkyldimetylamine oxides [43–45].

Fig. 6 depicts the electrolyte critical concentration (ECC), defined as the electrolyte concentration that marks the transition from shear thickening to shear thinning (i.e., the electrolyte concentration at which $I = 1$) versus the overall surfactant concentration. This diagram summarizes the complex rheological behavior and the structural changes observed in dilute CTAT micellar solutions containing the electrolytes examined. From this diagram, conditions for understanding the influence of C_D and ECC on the shear flow can be formulated: (i) at low electrolyte concentrations,

Table 1
Induction time, critical shear rate, power-law exponent m and critical deformation for 11 mmol/L CTAT micellar solutions containing 0.1 mmol/L electrolyte.

Electrolyte	$\dot{\gamma}_c$ (s^{-1})	Tind (s)	$\gamma(= \dot{\gamma}_c t_{ind,c})$	m
KBr	64	143	9406	-2.3 ± 0.30
$Na_2(COO)_2$	75	139	10,425	-2.6 ± 0.01
K_3PO_4	54	219	11,826	-2.1 ± 0.30
No electrolyte	94	106	9964	-3.2 ± 0.20

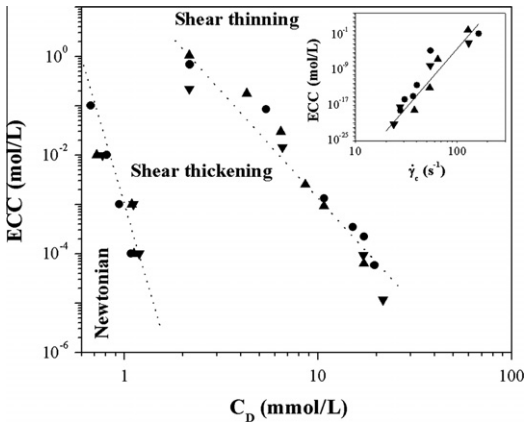

Fig. 6. Critical electrolyte concentrations as a function of the surfactant concentration for various salts: (●) KBr, (▲) $Na_2(COO)_2$ and (▼) K_3PO_4. The lines are only guides to the eye. Inset: ECC as a function of $\dot{\gamma}_c$.

below the ECC, shear thickening behavior dominates whereas at electrolyte concentrations larger than ECC, shear thinning behavior takes over at all CTAT concentrations within the dilute regime. More importantly, even though scattering in the data is evident, all of them can be fitted to a straight line regardless of electrolyte type, which indicates that ECC $\propto C_D^{\delta}$, with $\delta = -4.94 \pm 1.6$. Moreover, since the critical shear rate was found to depend on surfactant concentration as $\dot{\gamma}_c \propto C_D^{\alpha}$, it follows that ECC is roughly proportional to $\dot{\gamma}_c^{\delta/\alpha}$, which demonstrates that the ECC increases as the applied shear rate increases since both α and δ are negative (see inset in Fig. 6). The experimental exponent $\delta/\alpha = 4.3 \pm 0.4$ for the ECC as a function of $\dot{\gamma}_c$. In turn, this indicates that in the presence of electrolytes, smaller shear rates are required to induce shear thinning due to the micellar growth induced by the electrostatic screening.

In ionic surfactant solutions, micellar growth is promoted by electrostatic screening that reduces the repulsion between the charged polar headgroups upon addition of electrolytes [46] and/or by the reduction of the micellar surface charge density due to the addition of salts with strongly binding counterions [47,48], which become incorporated within the amphiphilic interface. Both effects lead to a reduction of the surfactant packing parameter $(v/(L \cdot a_s)$; where v, L, and a_s are the volume, stretched length, and head group area of the amphiphilic molecule, respectively [46]. As a consequence, electrolytes decrease the overlap concentration c^* and hence, strongly modify the shear thickening behavior [12,15]. However, no clear trends are found in the literature on shear thickening of micellar solutions upon addition of electrolytes. In general, shear thickening tends to vanish as the electrolyte concentration increases and the intensity of shear thickening, I, goes to one [3,15,33,36], in agreement with results reported here.

Our results on the influence of electrolytes with different counterion valence on the rheological behavior of dilute CTAT micellar solutions indicate that even though electrostatic screening is important, no definite effects of the type of counterion are noticeable. This suggests that when the surfactant has strongly binding counterions such as tosylate, electrostatic screening does not play the only role. The diagrams shown in Figs. 4 and 6 indicate that all the electrolytes, regardless of counterion valence, give similar effects on the transition from shear thickening to shear thinning behavior, which is a novel result. All the data fall effectively on general master curves. Moreover, we have shown that the transition from shear thickening to shear thinning is not abrupt but continuous, i.e., the shear thickening intensity goes smoothly to one as the surfactant or the electrolyte concentration increases, due to micellar growth.

4. Conclusions

Here the effects of adding various salts with increasing valence to the rheological behavior of CTAT micellar solutions were examined. This study was performed in the dilute concentration range, where shear thickening is observed for pure CTAT solutions. The induction time for the shear thickening and the magnitude of the viscosity growth as functions of shear rate or deformation depend strongly on the surfactant concentration. Also, the critical shear rate for the viscosity growth can be correlated with surfactant concentration (Fig. 5) and with electrolyte concentration (Fig. 6). The induction time was found to decrease strongly with the shear rate when the surfactant and electrolyte concentrations are fixed, according to a power-law with exponents from -2 to -4. It was also found that for the development of shear thickening, not only a critical shear rate is required but also a critical deformation (Table 1), which is a novel result.

Our data with CTAT and other data taken from the literature [3,33,36,37] indicate that the diagram shown in Fig. 4 may be a general one that allows explaining the mechanism controlling the type of observed rheological behavior. In this diagram, the mechanisms that determine shear thickening, the transition to shear thinning and the disappearance of shear thickening upon addition of electrolyte on surfactant micelles with strongly bound counterions are explained. Moreover, we found that the critical shear rate displays a power-law dependence on surfactant and electrolyte concentrations (see Fig. 5). Furthermore, the electrolyte critical concentration (ECC) also follows a power-law dependence on the critical shear rate ($\mathrm{ECC} \propto \dot{\gamma}_c^{\delta/\alpha} = \dot{\gamma}_c^{-4.9}$). This indicates that in the presence of electrolytes, smaller shear rates are required to induce shear thinning due to the growth of the micelles caused by the electrostatic screening and the underlying chemical equilibrium process. The rather insensitive behavior of the rheological behavior of dilute CTAT solutions on the type of added electrolyte can be explained by the strong binding of the tosylate counterion on the micelle surface, which renders it rather insensitive to variations of the outside electrostatic conditions. This finding is of relevance to the better understanding of such viscoelastic surfactant systems and in general for questions and applications where the control of flow properties of surfactant solutions is important.

Acknowledgments

We gratefully acknowledge DAAD-CONACyT Grant I110/2008 and PROALMEX (D/07/10253) for partial support of this work. We also thanks CONACyT (Project 100195) for the financial support.

References

[1] H. Rehage, H. Hoffman, J. Phys. Chem. 92 (1988) 4712.
[2] J.E. Puig, F. Bautista, J.F.A. Soltero, O. Manero, in: R. Zana, E.W. Kaler (Eds.), Giant Micelles: Structure and Properties, Taylor and Francis, New York, 2007.
[3] V. Hartmann, R. Cresseley, Europhys. Lett. 40 (1997) 691.
[4] J. Bender, N.J. Wagner, J. Rheol. 40 (1996) 899.
[5] D. Schuebel, Colloid Polym. Sci. 276 (1998) 743.
[6] R.L. Hoffmann, J. Rheol. 42 (1998) 111.
[7] Y. Séréro, V. Jacobsen, J.F. Berret, R. May, Macromolecules 33 (2000) 1841.
[8] Y.T. Hu, P. Boltenhagen, D.J. Pine, J. Rheol. 42 (1998) 1185.
[9] J.F. Berret, S. Lerouge, J.P. Decruppe, Langmuir 18 (2002) 7279.
[10] E.R. Macías, F. Bautista, J.F.A. Soltero, J.E. Puig, P. Attané, O. Manero, J. Rheol. 47 (2003) 643.
[11] V. Weber, F. Schosseler, Langmuir 18 (2002) 9705.
[12] C. Oelschlaeger, G. Waton, E. Buhler, S.J. Candau, M.E. Cates, Langmuir 18 (2002) 3076.
[13] J.F. Berret, R. Gámez-Corrales, S. Lerouge, J.P. Decruppe, Eur. Phys. J. E 2 (2000) 343.
[14] Y. Hu, S.Q. Wang, A.M. Jamieson, J. Rheol. 37 (1993) 531.
[15] W.J. Kim, S.-M. Yang, Langmuir 16 (2000) 6084.
[16] J. Dehmoune, J.-P. Decruppe, O. Greffier, H. Xu, Rheol. Acta.
[17] J. Dehmoune, J.-P. Decruppe, O. Greffier, H. Xu, J. Rheol. 52 (2008) 923.
[18] E.R. Macías, A. González, O. Manero, R. González-Nuñez, J.F.A. Soltero, P. Attané, J. Non-Newtonian Fluid Mech. 101 (2001) 149.
[19] R. Bandyopadhyay, A.K. Sood, Europhys. Lett. 56 (2001) 447.
[20] V. Herle, P. Fischer, E.J. Windhab, Langmuir 21 (2005) 9051.
[21] B.M. Marín-Santibañez, J. Pérez-González, L. de Vargas, F. Rodríguez-González, G. Huelsz, Langmuir 22 (2006) 4015.
[22] Y.T. Hu, P. Boltenhagen, E. Mathys, D.J. Pine, J. Rheol. 42 (1998) 1209.
[23] J.F. Berret, R. Gamez-Corrales, Y. Séréro, F. Molino, P. Lindner, Europhys. Lett. 54 (2001) 605.
[24] H. Rehage, H. Hoffmann, Mol. Phys. 74 (1991) 933.
[25] H. Hoffmann, in: C.A. Herb, R. Prudhomme (Eds.), Structure and Flow in Surfactant Solutions, ACS Symp. Ser. 578, ACS, Washington, DC, 1994, p. 2–31.
[26] A. Patist, J.R. Kanicky, P.K. Shukla, D.O. Shah, J. Colloid Interface Sci. 245 (2002) 1.
[27] Y. Rharbi, L. Chen, M.A. Winnik, J. Am. Chem. Soc. 126 (2004) 6025.
[28] A. Mohanty, T. Patra, I. Dey, J. Phys. Chem. B 111 (2007) 7155.
[29] A. Renoncourt, N. Vlachy, P. Bauduin, M. Drechsler, D. Touraud, J.M. Verbavatz, M. Dubois, W. Kunz, B.W. Ninham, Langmuir 23 (2007) 2376.
[30] S. Hoffmann, A. Rauscher, H. Hoffmann, Ber. Bunsen. Phys. Chem. 95 (1991) 153.
[31] J.F.A. Soltero, J.E. Puig, O. Manero, P.C. Schulz, Langmuir 11 (1995) 3337.
[32] J.F.A. Soltero, J.G. Álvarez-Ramírez, V.V.A. Fernández, N. Tepale, F. Bautista, E.R. Macías, J.H. Pérez-López, O. Manero, P.C. Schulz, C. Solans, J.E. Puig, J. Colloid Interface Sci. 312 (2007) 130.
[33] M.F. Torres, J.M. González, M.R. Rojas, A.J. Müller, A.E. Sáez, D. Lof, K. Schillen, J. Colloid Interface Sci. 307 (2007) 221.
[34] V. Hartmann, R. Cresseley, Colloids Surf., A 121 (1997) 151.
[35] V. Hartmann, R. Cresseley, Colloid Polym. Sci. 276 (1998) 169.
[36] M.T. Truong, L.M. Walker, Langmuir 18 (2002) 2024.
[37] C. Oelschlaeger, G. Waton, S.J. Candau, M.E. Cates, Langmuir 18 (2000) 7265.
[38] J.I. Escalante, E.R. Macías, F. Bautista, J.H. Pérez-López, J.F.A. Soltero, J.E. Puig, O. Manero, Langmuir 19 (2003) 6620.
[39] M. Takeda, T. Kusano, T. Matsunaga, H. Endo, M. Shibayama, T. Shikata, Langmuir 27 (2011) 1731.
[40] J.F. Berret, R. Gámez-Corrales, J. Oberdise, L.M. Walker, P. Lindner, Europhys. Lett. 41 (1998) 677.
[41] K. Sung, M.S. Han, C. Kim, Korea-Australia Rheol. J. 15 (2003) 151.
[42] R. Gámez-Corrales, J.F. Berret, L.M. Walker, J. Oberdisse, Langmuir 15 (1999) 6755.
[43] J.I. Escalante, H. Hoffmann, J. Phys. Condens. Matter 12 (2000) 483.
[44] J.I. Escalante, H. Hoffmann, Rheol. Acta 39 (2000) 209.
[45] J.I. Escalante, M. Gradzielski, H. Hoffmann, K. Mortensen, Langmuir 16 (2000) 8653.
[46] J.N. Israelachvili, Intermolecular and Surface Forces, Academic Press, Amsterdam, Holanda, 1992.
[47] P.A. Hassan, J.V. Yakhmi, Langmuir 16 (2000) 7187.
[48] P.A. Hassan, R.S. Raghavan, E.W. Kaler, Langmuir 18 (2002) 2543.